Geophysical Research Letters

RESEARCH LETTER
10.1029/2023GL105600

Infrared Radiative Effects of Increasing CO_2 and CH_4 on the Atmosphere in Antarctica Compared to the Arctic

Justus Notholt[1], Holger Schmithüsen[2], Matthias Buschmann[1], and Axel Kleidon[3]

[1]Institute of Environmental Physics, University of Bremen, Bremen, Germany, [2]Alfred-Wegener-Institute for Polar and Marine Research, Bremerhaven, Germany, [3]Max Planck Institute for Biogeochemistry, Jena, Germany

Key Points:

- We simulate the temperature development in both polar regions in the infrared and find that doubling CO_2 and CH_4 lead to opposing forcings
- The different amount of water vapor shows to be responsible for the differences in warming/cooling in both polar regions
- In Antarctica doubling CH_4 leads to a cooling of almost the whole troposphere, a future increase in H_2O could invert this

Supporting Information:

Supporting Information may be found in the online version of this article.

Correspondence to:

J. Notholt,
notholt@uni-bremen.de

Citation:

Notholt, J., Schmithüsen, H., Buschmann, M., & Kleidon, A. (2024). Infrared radiative effects of increasing CO_2 and CH_4 on the atmosphere in Antarctica compared to the Arctic. *Geophysical Research Letters*, *51*, e2023GL105600. https://doi.org/10.1029/2023GL105600

Received 20 JUL 2023
Accepted 30 NOV 2023

Author Contributions:

Conceptualization: Justus Notholt
Formal analysis: Matthias Buschmann
Funding acquisition: Justus Notholt
Investigation: Justus Notholt, Holger Schmithüsen
Methodology: Justus Notholt, Holger Schmithüsen
Software: Justus Notholt, Holger Schmithüsen
Visualization: Matthias Buschmann
Writing – original draft: Justus Notholt, Holger Schmithüsen

Abstract We simulated the seasonal temperature evolution in the atmosphere of Antarctica and the Arctic focusing on infrared processes. Contributions by other processes were parametrized and kept fixed throughout the simulations. The model was run for current CO_2 and CH_4 and for doubled concentrations. For doubling CH_4 the warming in Antarctica is restricted to the lowest few hundred meters above the surface while in the Arctic we find a warming in the whole troposphere. We find that the amount of water is the main driver for the differences between both polar regions. When increasing both, CO_2 and CH_4 from pre-industrial values to current concentrations, and averaged over the whole troposphere, we find a warming of 0.42 K for the Arctic and a slight cooling of 0.01 K for Antarctica. Our results contribute to the understanding of the lack of warming seen in Antarctica throughout the last decades.

Plain Language Summary In 2015 we have initiated a discussion on a fundamental property of the radiation in the atmosphere over Antarctica: The negative greenhouse effect (Schmithüsen et al., 2015, https://doi.org/10.1002/2015GL066749). A negative greenhouse effect means, the atmosphere emits more radiation to space than it receives from the surface. This results in a cooling somewhere in the Antarctic atmosphere during some months of the year, when increasing CO_2. We now simulate how the Antarctic atmospheric temperature responds in all altitude levels to CO_2 and CH_4 increases, and show this is different from the temperature response in the Arctic. We show for example, that an increase in CH_4 cools nearly the whole troposphere, although the response for CH_4 is much lower in amplitude than for CO_2. We find that the amount of water is the main driver for the differences between both polar regions. Since the amount of water vapor strongly depends on temperature, the colder Antarctic atmosphere responds differently to the Arctic when greenhouse gases increase. Our studies could be one important factor when understanding the lack of warming in Antarctica throughout the last decades.

1. Introduction

While the increase in greenhouse gases throughout the last decades has led to a strong warming in the Arctic, Antarctica reveals in parts a lack of warming. Several mechanisms have been proposed to explain this lack of warming and the delayed Antarctic sea-ice decline. These mechanisms include meteorological contributions and radiative effects (Holland et al., 2017; Kostov et al., 2018; Shindell & Schmidt, 2004; Shine & Forster, 1999), sea-ice transport changes (Haumann et al., 2016; Sun & Eisenman, 2021), changes in the deep ocean convection (de Lavergne et al., 2014; Latif et al., 2013), meltwater contributions (Bronselaer et al., 2018) and contributions from the tropics (Meehl et al., 2016). Recently (Rackow et al., 2022) studies of the sea-ice decline using high resolution climate models argue that one reason for the lack of warming is a more efficient ocean circulation that increases the equator-ward heat transport response to global warming, moderating the anthropogenic warming around Antarctica and thus delaying the sea-ice decline. Our studies contribute to the ongoing discussion on the conceptual explanation of the lack of warming in Antarctica.

CO_2 and CH_4 are the strongest forcing agents of anthropogenic climate change (Arias et al., 2021, Figure TS.15). As the surface is generally warmer than the atmosphere, an increase in greenhouse gas concentrations leads to a decrease in the transfer of infrared radiation from the surface to space (Schmithüsen et al., 2015). This is due to the fact that additional absorption in the atmosphere shields the (warm) surface emission from being emitted into space, while the associated re-emission into space is emitted by the (cold) atmosphere. This can be quantitatively studied by investigating the greenhouse effect, defined as the difference between the upward radiation from the surface and the radiation at the top of atmosphere to space (Thomas & Stamnes, 1999). While the greenhouse

effect normally increases for an increase in greenhouse gases, we could show in our previous study that for the high and cold elevated areas of central Antarctica a negative greenhouse effect is observed (Schmithüsen et al., 2015). A negative greenhouse effect means, the atmosphere emits more energy to space than it receives from the surface, leading to net-cooling of the atmospheric column. In the meantime, our observations have been confirmed by others (Chen et al., 2023; Freese & Cronin, 2021; Sejas et al., 2018; Smith et al., 2018). In Schmithüsen et al. (2015) we concentrated on CO_2 as originator for the negative greenhouse effect, later Sejas et al. (2018) pointed out that the effect of H_2O actually exceeds that of CO_2 in this respect. The occurrence of a negative greenhouse effect depends on the temperature profile and the distribution of the constituent in question. For instance, for CO_2 the relation between stratospheric and surface temperature is of relevance, but for H_2O the presence and intensity of a surface inversion determines the sign of the greenhouse effect. In fact, most relevant greenhouse gases can cause a negative greenhouse effect: when a strongly emitting atmospheric layer that can radiate into space is warmer than the surface the greenhouse effect can become negative. The potential of other greenhouse gases (namely O_3, CH_4, N_2O) in this respect can be seen in Schmithüsen (2015, Figure 2.1).

Our single column model used in our first study did not allow to investigate where in the atmosphere the cooling takes place and whether the negative greenhouse effect leads to a cooling of the surface in Antarctica. We have now extended our model to simulate the radiation and temperature development for all atmospheric layers and at the surface as a function of the atmospheric composition. The atmospheric temperature is determined by many factors, including the radiation in the ultraviolet/visible (UV/Vis) and in the infrared spectral region, the effects of clouds, advection, convection, and feedback processes. Since the warming/cooling by greenhouse gases occurs mainly in the infrared spectral region we restricted our studies to that region. All other processes determining the temperature development, mentioned above, were included as constant averages we name ΔT_{res}, calculated as described below. This allowed us to perform process studies to investigate only the first-order impact of specific greenhouse gas concentrations on the temperature development. In order to avoid uncertainties of broad-band radiation parametrizations our simulations were done using a high resolution model (0.01 cm^{-1}, i.e., line-by-line), based on Notholt et al. (2006).

In a first step we simulated the annual temperature cycle in Antarctica and the Arctic for current greenhouse gas concentrations (CO_2: 400 ppmv denoted "1xCO_2"; CH_4: 1.85 ppmv in the troposphere, decreasing above denoted "1xCH_4"; H_2O: based on ERA5 denoted "1xH_2O") and compared the results to temperature profiles deduced from ERA-5 reanalysis data. In the second step we run the simulations with 2xCO_2 or 2xCH_4. The difference between the corresponding simulations gives us the induced warming/cooling in each atmospheric layer and the surface throughout the year. In order to investigate the role of H_2O in detail we also run the simulations with 2xCO_2 and 2xCH_4 for Antarctica with strongly increased water vapor (5xH_2O, comparable to the Arctic) and with strongly decreased water vapor (0.2xH_2O) for the Arctic, comparable to Antarctica.

2. Methods

2.1. Calculation of the Temperature Development for Current CO_2 and CH_4 Mixing Ratios

Our model is based on our line-by-line code described in Notholt et al. (2006). It has been modified to calculate the radiation and temperature development in high resolution (0.01 cm^{-1}) in each of the 90 atmospheric layers in the spectral region 50 to 2,000 cm^{-1} (5–200 μm).

From monthly averaged ECMWF reanalysis data (ERA5) at 90°N or 90°S (Muñoz Sabater, 2019) we derived 12 temperature profiles as climatological average over 30 years (1990–2020); above ∼60 km the profiles are complemented by the US-standard atmosphere. The volume mixing ratios of all trace gases other than CO_2, CH_4, H_2O and O_3 are based on long-term averages from balloon soundings and satellite data originating from the Upper Atmospheric Research Satellite Correlative Measurements Program (UARS-CMP) (Peterson & Margitan, 1995). The data from the 12 monthly averaged temperature, H_2O and O_3 profiles were spline (piecewise cubic polynomial fit) interpolated to each individual time of the simulation. The method based on monthly averages was chosen in order to simulate a smooth annual cycle that still features the predominant seasonal temperature evolution throughout the year. For consecutive years of the simulation the same 12 profiles for temperature, H_2O and O_3 were used. Spectral data were taken from the HITRAN2008 (Rothman et al., 2009) and HITRAN2012 (Rothman et al., 2013) molecular spectroscopic databases and the ATM2019 linelist (https://mark4sun.jpl.nasa.gov/specdata.html). The line broadening was calculated using a Voigt profile (Humlicek, 1982). The H_2O and CO_2 continuum was added, using the MT_CKD model (Mlawer et al., 2012).

Our program calculates the infrared radiation. In order to get the total atmospheric energy budget, contributions by for example, solar UV/Vis radiation, advection, clouds, convection, and feedback processes, need to be considered. We pre-calculate the sum of these contributions as difference between our long-wave simulation and a climatological temperature evolution based on ERA5 and name them temperature residuals $\Delta T_{res}(z, t)$ as described below.

Using a starting temperature profile our model gives the upward and downward radiation in every altitude layer. The radiation together with the heat capacity of each layer gives for each altitude z and time step Δt the long-wave change in temperature $\Delta T_{LW}(z, t)$. The difference between the real temperature change $\Delta T(z, t)$, from the spline interpolated ERA5 data and the simulated temperature change $\Delta T_{LW}(z, t)$ can be assigned to contributions by all other processes mentioned above, $\Delta T_{res}(z, t)$.

$$\Delta T(z,t) \; - \; \Delta T_{\mathrm{LW}}(z,t) =: \; \Delta T_{\mathrm{res}}(z,t) \tag{1}$$

The residuals $\Delta T_{res}(z, t)$ have been calculated for all layers in the atmosphere for each month (12 profiles) and are prescribed input to the model experiments. As the heat capacity of the surface ($z = z_0$) cannot be calculated directly a substitute "surface sensitivity" is used (see Supporting Information S1).

The temperature development after a time step Δt for the new temperature $T(t + \Delta t)$ can now be calculated as

$$T(z,t+\Delta t) = T(z,t) + \Delta T_{\mathrm{LW}}(z,t) + \Delta T_{\mathrm{res}}(z,t) \tag{2}$$

Using a starting profile (1 January in Antarctica; 1 July in the Arctic), the temperature change from the infrared simulation $\Delta T_{LW}(z, t)$ is added to the previous temperature $T(z, t)$, corrected with $\Delta T_{res}(z, t)$, spline interpolated from the prescribed monthly $\Delta T_{res}(z, t)$ profiles for the specific time of the year. The model runs were done for a time step Δt of 3 hrs in Antarctica and 1 hr for the Arctic, for longer time steps the calculated temperatures started to oscillate. Figure S1 in Supporting Information S1 gives an example for $\Delta T_{res}(z, t)$, $\Delta T_{LW}(z, t)$ and $\Delta T(z, t)$.

The difference between the ERA5-based input profiles and our simulated temperatures is within a range of ±0.1 to ±0.2 K or better (Figure S2 in Supporting Information S1). The variability is due to the use of monthly calculated $\Delta T_{res}(z, \Delta t)$ and the numerical effects of the interpolation. Since we are interested in the seasonal temperature development the differences for the short term variability is not of importance. When averaging for longer periods of a few months the ERA5-data and our simulated temperatures agree within much less than ±0.05 K. This means, our simulated annual temperature cycle agrees well with the ERA5 data. We would like to point out that only one starting temperature profile has been used to simulate the temperature development for the whole year or longer, while the model is nudged by the pre-calculated temperature residuals.

2.2. Calculation of Warming/Cooling for Doubling CO_2 and CH_4

In the first step the simulations were performed for current concentrations of CO_2 and CH_4, using the prescribed ΔT_{res}. In the next step the simulations were repeated for $2xCO_2$ or $2xCH_4$. We used the same prescribed residuals ΔT_{res} from above, calculated for $1xCO_2$ and $1xCH_4$. This allowed us to identify the contribution caused by the change in the infrared radiation separated from all other processes. In order to allow the simulations to reach equilibrium for the enhanced greenhouse gas concentrations we calculated the temperature development for a period of 3 years. We consider equilibrium to be reached once the year-to-year variation of the temperature is constantly below 0.01 K. The results shown in the next paragraphs are for year three.

Since the main infrared absorbers are H_2O, CO_2, CH_4, N_2O, and O_3 we used only these five trace gases for our simulations in order to speed up the calculations. Test runs with all 52 infrared active trace gases show an excellent agreement to within 0.01 K (Figure S3 in Supporting Information S1).

We have also applied our program to the US-Standard atmosphere (Figure S4 in Supporting Information S1). For $2xCO_2$ we find a temperature increase of 2.2 K at 2 m altitude, in good agreement with 1.95 K that can be concluded from the studies by Gillett et al. (2013) using global climate models. For these runs the water vapor feedback was considered, which means, the relative humidity was kept constant during the temperature evolution.

3. Results

Figures 1a and 1c show the resulting temperature differences between the simulations with $2xCO_2$ and $1xCO_2$. Figures 1b and 1d give the results for $2xCH_4$–$1xCH_4$. Results are shown for absolute altitudes up to 12 km, Figure

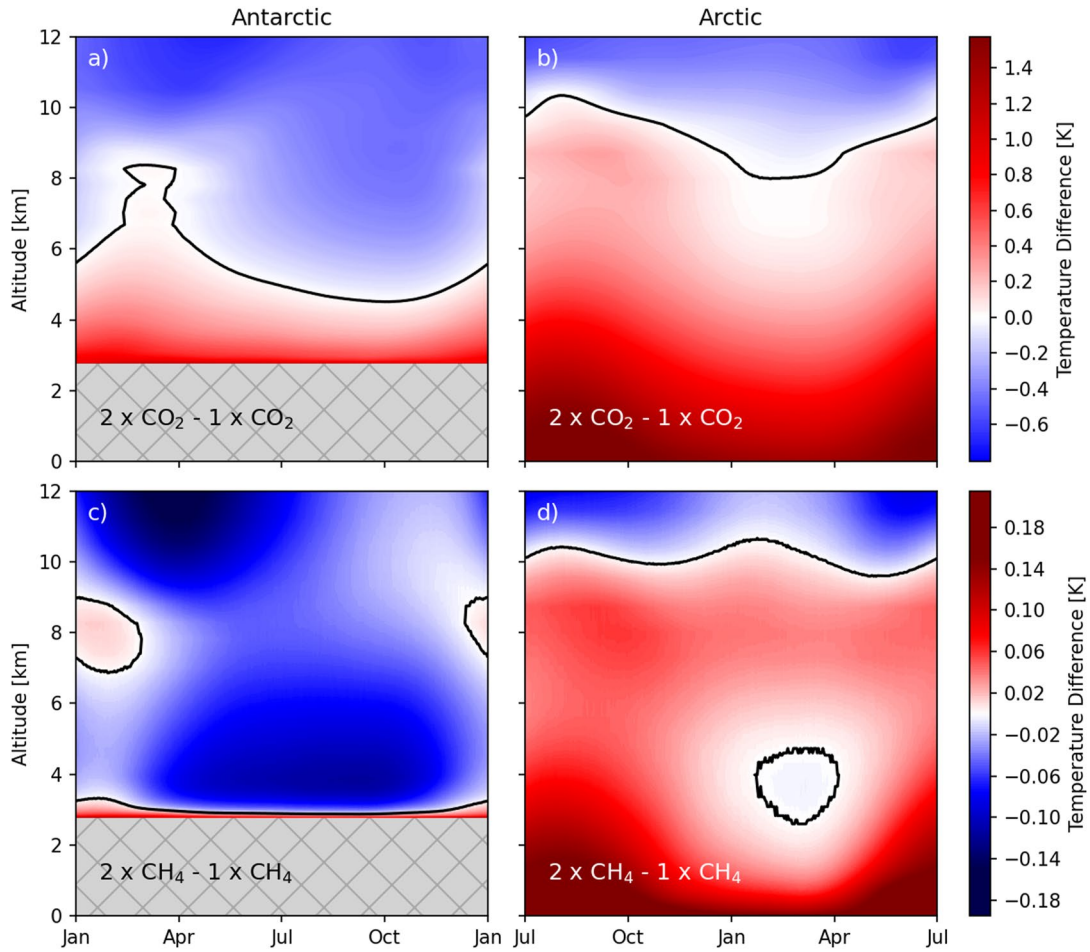

Figure 1. Temperature forcing (K) as a function of altitude throughout the year calculated for $2xCO_2$–$1xCO_2$ (a and c) and $2xCH_4$–$1xCH_4$ (b and d) for Antarctica (a and c) and the Arctic (b and d). In Antarctica the surface is at 2.8 km altitude, in the Arctic at 1 m.

S5 in Supporting Information S1 gives the corresponding results up to 90 km. When doubling CO_2 the troposphere in Antarctica shows a warming from the surface at 2.8 km altitude up to 5.5 km on average and a cooling above (Figure 1a). In the Arctic we find a warming from the surface at 0 km altitude essentially up to tropopause (8.4 km on average) and cooling above (Figure 1b). When doubling CH_4 the warming in Antarctica is restricted to the first 100–400 m above the surface at 2.8 km (the first 10–20 layers in the model, Figure 1c). Above, the atmosphere cools, except a slight warming at 8 km in January and February. For the Arctic the warming by CH_4 is found up to 10 km on average, with the exception of a slight cooling around 3–4 km around February (Figure 1d). Note that the model setup does not allow for changes in vertical or horizontal airmass mixing, or non-radiative feedback processes. Hence, any temperature signals shown are solely due to the forcing from the change in CO_2 or CH_4. In reality, vertical and horizontal mixing would smooth the temperature signals.

As shown by Dufresne et al. (2020) the negative greenhouse effect of CO_2 depends on the spectral overlap with other greenhouse gases, particularly H_2O. This effect can be seen when reducing the H_2O concentration of the Arctic profiles in our simulations to 20%, comparable to Antarctica, or increasing the water content in Antarctica by a factor of 5, comparable to the Arctic conditions (Figure S6 in Supporting Information S1 shows typical H_2O profiles). Results from these simulations are shown in Figure 2. We would like to point out that a 5× higher water amount is probably unrealistic, the water concentration could then be higher than the saturation pressure of H_2O, but in our case it is a useful sensitivity study.

When reducing H_2O in the Arctic to 20% we find a comparable temperature pattern forcing for $2xCH_4$ as for Antarctica (compare Figure 2d with Figure 1c). The warming then remains restricted to the lowest troposphere, and a cooling is observed above. A corresponding effect is visible when increasing the water content in Antarctica

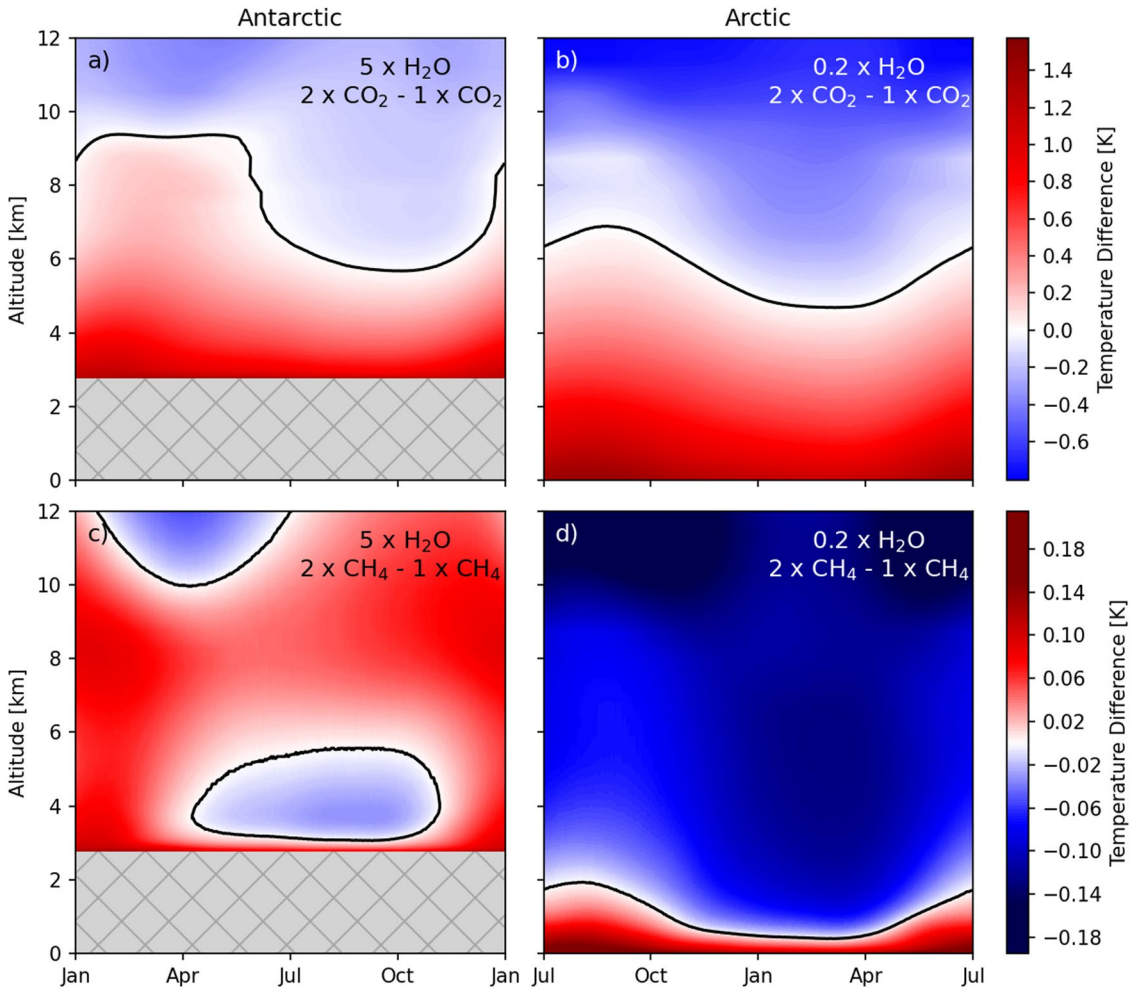

Figure 2. Test simulations for Antarctica (a) and (c) and the Arctic (b) and (d). Shown is ΔT between two runs, simulated for $2xCO_2$–$1xCO_2$, (a) and (b) with 5 times H_2O for Antarctica (a) and 20% water in the Arctic (b). Panels (c) and (d) give the same test runs for $2xCH_4$–$1xCH_4$.

by a factor of 5, leading to a much stronger warming for $2xCH_4$, comparable to the Arctic (compare Figure 2c with Figure 1d), with a warming nearly throughout the whole troposphere. Similarly, for CO_2 we see less warming of the troposphere when reducing water in the Arctic to 20% (compare Figure 2b with Figure 1b) and increased warming for 5 times H_2O in Antarctica (Figure 2a compare to Figure 1a). Interestingly, for 5 times H_2O Antarctica shows a slight cooling for $2xCH_4$ above the surface in winter (June to August) which coincides with the strongest surface inversions in the respective model setups.

4. Discussion

In general, when increasing the concentration of a uniformly distributed greenhouse gas, the lower atmosphere gets warmer, above a cooling results. The altitude where a warming switches to a cooling we name $z_{w/c}$. The warming in the lower atmosphere results from the increased insulating effect of greenhouse gases and the increased downwards radiation from the atmosphere above (Dufresne et al., 2020). The strong absorption by for example, tropospheric H_2O masks the emission by the surface. The top-of-atmosphere radiative loss originates from within the atmosphere, the effective emission height is determined by the amount of H_2O. The cooling above $z_{w/c}$ results from the increased upward radiative loss to space.

Figure 3a shows the longwave downwards and upwards radiation for current mixing ratios of CO_2 and CH_4 ($1xCO_2$ and $1xCH_4$) in Antarctica. The dotted lines give the radiation when increasing the amount of water by a factor of 5. For enhanced H_2O the longwave downwards radiation increases within the troposphere, shifting $z_{w/c}$

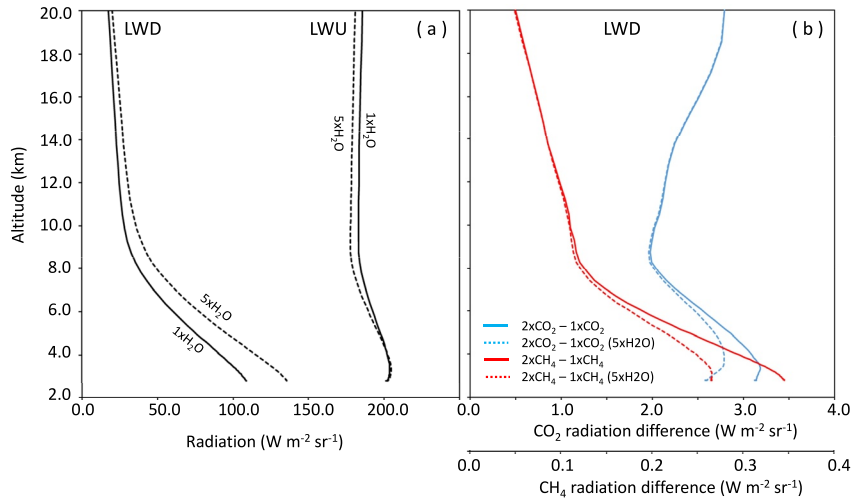

Figure 3. (a) LWD and LWU for current CO_2 and CH_4 mixing ratios over Antarctica. The dotted lines give the results for 5 times H_2O. (b) Difference in LWD for $2xCO_2$–$2xCO_22$ and $2xCH_4$–$1xCH_4$ for Antarctica. The dotted lines give the results for 5 times H_2O. Note the different scaling for CO_2 and CH_4.

to a higher altitude. At the same time, the upwards radiation for $5xH_2O$ slightly decreases, because the emission is coming from higher up in the atmosphere, where it is colder. The Figure documents in general the increase in $z_{w/c}$ for increasing H_2O.

Figure 3b shows the difference in the longwave downwards radiation for $2xCO_2$–$1xCO_2$ and $2xCH_4$–$1xCH_4$. Note the different scaling for both trace gases. While CO_2 has a nearly constant mixing ratio throughout the whole atmosphere, the mixing ratio of CH_4 decreases with altitude. This is reflected in the radiation difference in the stratosphere which increases with altitude for $2xCO_2$–$1xCO_2$ while it decreases for $2xCH_4$–$1xCH_4$. This increase in the downwards radiation above the tropopause leads to the well-known warming of the troposphere. Since the stratospheric mixing ratio profiles of CO_2 and CH_4 qualitatively differ, the resulting warming of the troposphere for increased downwards radiation of CO_2 and CH_4 differ. The dotted lines in Figure 3b give the results for 5-times H_2O. For the increased H_2O the radiation difference decreases, caused by the masking effect of H_2O.

Tropospheric heating caused by increasing greenhouse gases is directly coupled to increasing stratospheric downwards radiation. Sensitivity studies by doubling the mixing ratios of CH_4 or CO_2 only in the upper troposphere and stratosphere confirm the role of the downward radiation from the upper troposphere/stratosphere (Figure S7 in Supporting Information S1). If a greenhouse gas is only increasing in the troposphere, the level $z_{w/c}$ lowers significantly (Figures S7a and S7b in Supporting Information S1). Since for CH_4 a doubling influences the troposphere more than the stratosphere due to its decrease in mixing ratio with altitude, $z_{w/c}$ lowers accordingly. We conclude that the difference in the mixing ratio profiles is mainly responsible for the difference in $z_{w/c}$ between CO_2 compared to CH_4.

Our studies confirm previous results (Chen et al., 2023; Dufresne et al., 2020; Sejas et al., 2018) that the amount of water is the dominant factor for the different temperature forcings when comparing Arctic and Antarctic. We also investigated how CH_4 behaves compared to CO_2. The altitude $z_{w/c}$, where the warming switches to a cooling differs, depending on the mixing ratio profiles of both trace gases. Our simulations with 5 times water for Antarctica and 0.2 times water for the Arctic further demonstrate that the specific temperature profiles in Antarctica, with sometimes higher temperatures in the stratosphere compared to the surface, are only of minor importance.

Comparing the simulated temperatures of current CO_2 and CH_4 concentrations (400 ppm CO_2 and 1.85 ppm CH_4) to pre-industrial values (278 ppm CO_2 and 0.75 ppm CH_4) results in an overall slight warming only in the first 1–2 km above the surface in Antarctica (Figure 4a). While the overall warming in Antarctica is limited to up to 4–5 km, the warming in the Arctic takes place up to 8–9 km (Figure 4b).

We have calculated the pressure weighted average of the simulated temperature changes up to 7,000 m for doubling CO_2 and CH_4 (Table 1). The overall temperature increase up to 7,000 m in the Arctic for doubling CO_2

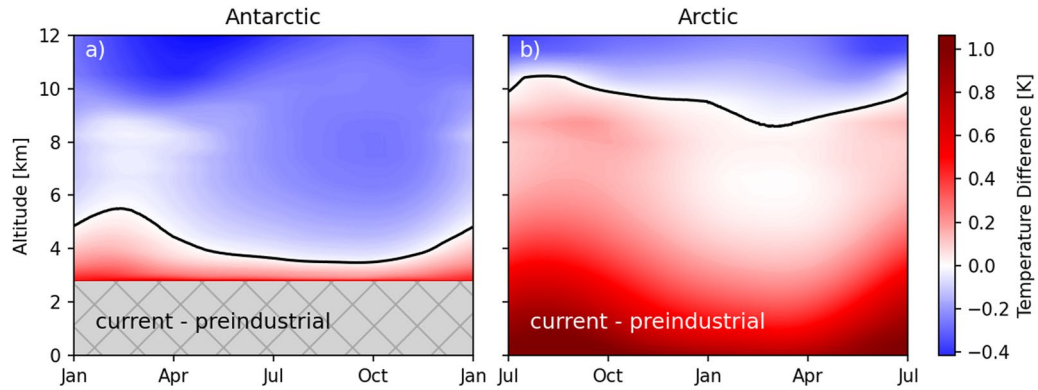

Figure 4. Temperature forcing as a function of altitude throughout the year calculated for the comparison of current greenhouse gas concentrations (400 ppm CO_2 and 1.85 ppm CH_4) versus pre-industrial values (278 ppm CO_2 and 0.75 ppm CH_4) for Antarctica (a) and the Arctic (b). In Antarctica the surface is at 2.8 km altitude, in the Arctic at 1 m.

with 0.81 K is much higher than what we get for Antarctica (0.16 K). For a doubling of CH_4, in Antarctica a slight cooling of 0.06 K results compared to a warming of 0.07 K for the Arctic, when averaging up to 7,000 m. When increasing both, CO_2 and CH_4 from pre-industrial values to the current concentrations results in a warming of 0.42 K for the Arctic and 0.02 K for Antarctica.

5. Conclusions

Our studies yield the instantaneous forcing when doubling CO_2 or CH_4. Changes in vertical or horizontal mixing following a warming or cooling are not considered. In reality the temperature signals would smooth out. In our simulations for Antarctica we find a cooling for doubling CH_4 nearly throughout the whole troposphere, but not at the surface or in the first 100–500 m above the surface. For doubling CO_2 the Antarctic atmosphere shows a warming up to 5.5 km and cooling above. Mixing processes might lead to a slight cooling at the surface in Antarctica. Overall, other feedback processes are important for the observed temperature increases in both polar regions. While we calculated a warming of 0.95 K since pre-industrial CO_2 and CH_4 for the Arctic, the observed increase since 1960 is 2–3 K (Wendisch et al., 2023). The difference results from the various feedback processes, most importantly the melt of sea ice and the lapse rate feedback (Pithan & Mauritsen, 2014).

Table 1
Temperature Change (K) for 2xCO_2–1xCO_2, 2xCH_4–1xCH_4, and Current CO_2 and CH_4 Pre-Industrial Values, Averaged for the Atmosphere From the Surface up to 7 km Altitude and Given at 2 m Altitude

	2xCO_2–1xCO_2	2xCH_4–1xCH_4	Current–pre-industrial
Arctic			
0–7,000 m	0.81	0.07	0.42
2 m	1.53	0.19	0.95
Antarctica			
0–7,000 m	0.16	−0.06	0.02
2 m	1.02	0.07	0.58

Our studies demonstrate that the Antarctic atmosphere is much less prone to direct radiative heating compared to the Arctic. This study could be one piece in the puzzle when understanding the lack of warming in Antarctica throughout the last decades compared to the Arctic.

Our findings are in line with Sejas et al. (2018), who concluded that for the Arctic a colder climate in the past would imply drier conditions, with a potential for a negative greenhouse effect caused by surface inversions. Our results confirm this, and show that a colder and drier Arctic could have led to a cooling by an increase in CH_4, maintaining the cold Arctic climate conditions. In this way, our results suggest that for a sustained warming, and accompanied increase of H_2O, the cooling by CH_4 in the Antarctic troposphere might turn into a warming, corresponding to a tipping point in the Antarctic atmosphere. This might lead to an increase in the temperature in Antarctica.

Data Availability Statement

The LBL radiative transfer code is available at Notholt (2023a). The resulting data set used in this paper can be accessed at Notholt (2023b). The additional programs to calculate the model-observation comparison, the spline fitting routine and programs for creating the Figures are available at Schmithüsen et al. (2023).

Acknowledgments
We gratefully acknowledge Eli Mlawer for helpful discussions on the water vapour continuum model MT_CKD model. We gratefully acknowledge the funding by the Deutsche Forschungsgemeinschaft (DFG, German Research Foundation)–Projektnummer 268020496–TRR 172, within the Transregional Collaborative Research Center "ArctiC Amplification: Climate Relevant Atmospheric and SurfaCe Processes, and Feedback Mechanisms (AC)³".

References

Arias, P. A., Bellouin, N., Coppola, E., Jones, R. G., Krinner, G., Marotzke, J., et al. (2021). Technical summary. In V. Masson-Delmotte, P. Zhai, A. Pirani, S. L. Connors, C. Péan, S. Berger (Eds.), *Climate change 2021: The physical science basis. Contribution of working group I to the sixth assessment report of the Intergovernmental Panel on Climate Change* (pp. 33−144). Cambridge University Press. https://doi.org/10.1017/9781009157896.002

Bronselaer, B., Winton, M., Griffies, S. M., Hurlin, W. J., Rodgers, K. B., Sergienko, O. V., et al. (2018). Change in future climate due to Antarctic meltwater. *Nature*, *564*(7734), 53–58. https://doi.org/10.1038/s41586-018-0712-z

Chen, Y.-T., Huang, Y., & Merlis, T. M. (2023). The global patterns of instantaneous CO_2 forcing at the top of the atmosphere and the surface. *American Meteorological Society*, *36*(18), 6331–6347. https://doi.org/10.1175/JCLI-D-22-0708.1

de Lavergne, C., Palter, J. B., Galbraith, E. D., Bernardello, R., & Marinov, I. (2014). Cessation of deep convection in the open Southern Ocean under anthropogenic climate change. *Nature Climate Change*, *4*, 278–282. https://doi.org/10.1038/nclimate2132

Dufresne, J.-L., Eymet, V., Crevoisier, C., & Grandpeix, J.-Y. (2020). Greenhouse effect: The relative contributions of emission height and total absorption. *Journal of Climate*, *33*(9), 3827–3844. https://doi.org/10.1175/JCLI-D-19-0193.1

Freese, L. M., & Cronin, T. W. (2021). Antarctic radiative and temperature responses to a doubling of CO_2. *Geophysical Research Letters*, *48*(17), e2021GL093676. https://doi.org/10.1029/2021GL093676

Gillett, N. P., Arora, V. K., Matthews, D., & Allen, M. R. (2013). Constraining the ratio of global warming to cumulative CO_2 emissions using CMIP5 simulations. *Journal of Climate*, *26*(18), 6844–6858. https://doi.org/10.1175/JCLI-D-12-00476.1

Haumann, F. A., Gruber, N., Münnich, M., Frenger, I., & Kern, S. (2016). Sea-ice transport driving Southern Ocean salinity and its recent trends. *Nature*, *537*(7618), 89–92. https://doi.org/10.1038/nature19101

Holland, M. M., Landrum, L., Raphael, M., & Stammerjohn, S. (2017). Springtime winds drive Ross Sea ice variability and change in the following autumn. *Nature Communications*, *8*(1), 731. https://doi.org/10.1038/s41467-017-00820-0

Humlicek, J. (1982). Optimized computation of the Voigt and complex probability functions. *Journal of Quantitative Spectroscopy & Radiative Transfer*, *27*(4), 437–444. https://doi.org/10.1016/0022-4073(82)90078-4

Kostov, Y., Ferreira, D., Armour, K. C., & Marshall, J. (2018). Contributions of greenhouse gas forcing and the southern annular mode to historical Southern Ocean surface temperature trends. *Geophysical Research Letters*, *45*(2), 1086–1097. https://doi.org/10.1002/2017GL074964

Latif, M., Martin, T., & Park, W. (2013). Southern Ocean sector centennial climate variability and recent decadal trends. *Journal of Climate*, *26*(19), 7767–7782. https://doi.org/10.1175/JCLI-D-12-00281.1

Meehl, G. A., Arblaster, J. M., Bitz, C. M., Chung, C. T. Y., & Teng (2016). H. Antarctic sea-ice expansion between 2000 and 2014 driven by tropical Pacific decadal climate variability. *Nature Geoscience*, *9*, 590–596. https://doi.org/10.1038/ngeo2751

Mlawer, E. J., Payne, V. H., Moncet, J.-L., Delamere, J. S., Alvarado, M. J., & Tobin, D. C. (2012). Development and recent evaluation of the MT_CKD model of continuum absorption. *Philosophical Transactions of the Royal Society A*, *370*(1968), 2520–2556. https://doi.org/10.1098/rsta.2011.0295

Muñoz Sabater, J. (2019). ERA5-Land monthly averaged data from 1950 to present. *Copernicus Climate Change Service (C3S) Climate Data Store (CDS)*. https://doi.org/10.24381/cds.68d2bb30

Notholt, J. (2023a). Line-by-line code ILBL from 26 Aug 2022 (2022.08) [Software]. Zenodo. https://doi.org/10.5281/zenodo.8168114

Notholt, J. (2023b). Results on temperature development for 1xCO2, 2xCO2, and 2xCH_4 for Arctic and Antarctica (2023.07) [Dataset]. Zenodo. https://doi.org/10.5281/zenodo.8168233

Notholt, J., Toon, G., Jones, N., Griffith, D., & Warneke, T. (2006). Spectral line finding program for atmospheric remote sensing using full radiation transfer. *Journal of Quantitative Spectroscopy & Radiative Transfer*, *97*(1), 112–125. https://doi.org/10.1016/j.jqsrt.2004.12.025

Peterson, D. B., & Margitan, J. M. (1995). *Upper atmospheric research satellite Correlative measurements program (UARS-CMP), balloon data Atlas* (p. 214). National Aeronautics and Space Administration.

Pithan, F., & Mauritsen, T. (2014). Arctic amplification dominated by temperature feedbacks in contemporary climate models. *Nature Geoscience*, *7*(3), 181–184. https://doi.org/10.1038/ngeo2071

Rackow, T., Danilov, S., Goessling, H. F., Hellmer, H. H., Sein, D. V., Semmler, T., et al. (2022). Delayed Antarctic sea-ice decline in high-resolution climate change simulations. *Nature Communications*, *13*(1), 637. https://doi.org/10.1038/s41467-022-28259-y

Rothman, L. S., Gordon, I., Babikov, Y., Barbe, A., Chris Benner, D., Bernath, P., et al. (2013). The HITRAN2012 molecular spectroscopic database. *Journal of Quantitative Spectroscopy and Radiative Transfer*, *130*, 4–50. https://doi.org/10.1016/j.jqsrt.2013.07.002

Rothman, L. S., Gordon, I., Barbe, A., Benner, D., Bernath, P., Birk, M., et al. (2009). The HITRAN 2008 molecular spectroscopic database. *Journal of Quantitative Spectroscopy and Radiative Transfer*, *110*(9–10), 533–572. https://doi.org/10.1016/j.jqsrt.2009.02.013

Schmithüsen, H. (2015). Antarctic specific features of the greenhouse effect: A radiative analysis using measurements and models Dissertation. University of Bremen. Retrieved from http://nbn-resolving.de/urn:nbn:de:gbv:46-00104190-18

Schmithüsen, H., Buschmann, M., & Notholt, J. (2023). Additional programs for GRL paper [Software]. Zenodo. https://doi.org/10.5281/zenodo.10188701

Schmithüsen, H., Notholt, J., König-Langlo, G., Lemke, P., & Jung, T. (2015). How increasing CO_2 leads to an increased negative greenhouse effect in Antarctica. *Geophysical Research Letters*, *42*(23), 10422–10428. https://doi.org/10.1002/2015GL066749

Sejas, S. A., Taylor, P. C., & Cai, M. (2018). Unmasking the negative greenhouse effect over the Antarctic Plateau, Nature. *npj Climate and Atmospheric Science*, *1*, 17. https://doi.org/10.1038/s41612-018-0031-y

Shindell, D. T., & Schmidt, G. A. (2004). Southern Hemisphere climate response to ozone changes and greenhouse gas increases. *Geophysical Research Letters*, *31*(18), L18209. https://doi.org/10.1029/2004GL020724

Shine, K. P., & de Forster, P. M. F. (1999). The effect of human activity on radiative forcing of climate change: A review of recent developments. *Global and Planetary Change*, *20*(4), 205–225. https://doi.org/10.1029/1999RG000078

Smith, K. L., Chiodo, G., Previdi, M., & Polvani, L. M. (2018). No surface cooling over Antarctica from the negative greenhouse effect associated with instantaneous quadrupling of CO_2 concentrations. *Journal of Climate*, *31*(1), 317–323. https://doi.org/10.1175/JCLI-D-17-0418.1

Sun, S., & Eisenman, I. (2021). Observed Antarctic sea ice expansion reproduced in a climate model after correcting biases in sea ice drift velocity. *Nature Communications*, *12*(1), 1060. https://doi.org/10.1038/s41467-021-21412-z

Thomas, G. E., & Stamnes, K. (1999). *Radiative transfer in the atmosphere and ocean*. Cambridge University Press. https://doi.org/10.1017/CBO9780511613470

Wendisch, M., Brückner, M., Crewell, S., Ehrlich, A., Notholt, J., Lüpkes, C., et al. (2023). Atmospheric and surface processes, and feedback mechanisms determining Arctic amplification a review of first results and prospects of the (AC)3 project. *Bulletin America Meteorology Social*, *104*(1), 208–242. https://doi.org/10.1175/BAMS-D-21-0218.1

References From the Supporting Information

Pirazzini, R., Hannula, H.-R., Shupe, M. D., Uttal, T., Cox, C. J., Costa, D., et al. (2022). Upward and downward broadband shortwave and longwave irradiance and downward diffuse and direct solar partitioning during the MOSAiC expedition. *PANGAEA*. https://doi.org/10.1594/PANGAEA.952359

Riihimaki, L., Long, C. E., Dutton, E. G., & Michalsky, J. (2023). *Basic and other measurements of radiation at station South Pole (1992-01 et seq)*. NOAA Global Monitoring Laboratory. https://doi.org/10.1594/PANGAEA.956847